High-yield hydrogen production from biomass by in vitro metabolic engineering: Mixed sugars coutilization and kinetic modeling

Joseph A. Rollin[a,b], Julia Martin del Campo[a], Suwan Myung[a,c], Fangfang Sun[b], Chun You[a,b], Allison Bakovic[d], Roberto Castro[e], Sanjeev K. Chandrayan[f], Chang-Hao Wu[f], Michael W. W. Adams[f,g], Ryan S. Senger[a], and Y.-H. Percival Zhang[a,b,c,h,1]

[a]Department of Biological Systems Engineering, Virginia Tech, Blacksburg, VA 24061; [b]Cell-Free Bioinnovations, Blacksburg, VA 24060; [c]Institute for Critical Technology and Applied Science, Virginia Tech, Blacksburg, VA 24061; [d]Department of Physics and Chemistry, Milwaukee School of Engineering, Milwaukee, WI 53202; [e]Department of Chemical and Natural Gas Engineering, Texas A&M University, Kingsville, TX 78363; [f]Department of Biochemistry and Molecular Biology, University of Georgia, Athens, GA 30602; [g]Department of Energy BioEnergy Science Center, Oak Ridge, TN 37831; and [h]Tianjin Institute of Industrial Biotechnology, Chinese Academy of Sciences, Tianjin 300308, China

The use of hydrogen (H_2) as a fuel offers enhanced energy conversion efficiency and tremendous potential to decrease greenhouse gas emissions, but producing it in a distributed, carbon-neutral, low-cost manner requires new technologies. Herein we demonstrate the complete conversion of glucose and xylose from plant biomass to H_2 and CO_2 based on an in vitro synthetic enzymatic pathway. Glucose and xylose were simultaneously converted to H_2 with a yield of two H_2 per carbon, the maximum possible yield. Parameters of a nonlinear kinetic model were fitted with experimental data using a genetic algorithm, and a global sensitivity analysis was used to identify the enzymes that have the greatest impact on reaction rate and yield. After optimizing enzyme loadings using this model, volumetric H_2 productivity was increased 3-fold to 32 mmol $H_2 \cdot L^{-1} \cdot h^{-1}$. The productivity was further enhanced to 54 mmol $H_2 \cdot L^{-1} \cdot h^{-1}$ by increasing reaction temperature, substrate, and enzyme concentrations—an increase of 67-fold compared with the initial studies using this method. The production of hydrogen from locally produced biomass is a promising means to achieve global green energy production.

hydrogen | biomass | in vitro metabolic engineering | metabolic network modeling | global sensitivity analysis

Unlocking the tremendous potential of the hydrogen (H_2) economy depends on the availability of low-cost, distributed hydrogen produced in a carbon-neutral manner. Approximately 50 million metric tons of hydrogen produced from fossil fuels annually are used mainly for oil refining and ammonia synthesis (1). However, current thermochemical production options are prohibitively expensive, especially for distributed production systems, when infrastructure costs are considered (1, 2). Water electrolysis is scalable and potentially renewably powered, but this technology remains expensive (3). Water splitting powered by solar energy (4, 5) suffers from low solar-to-chemical energy conversion efficiencies and low volumetric productivities and is far from practical applications (5, 6). For the hydrogen economy to become reality, new technologies must be developed to meet increasing needs while keeping both production costs and capital costs low and simultaneously reducing greenhouse gas emissions (7).

Biomass is the most abundant renewable resource and is far more evenly distributed worldwide than fossil fuels. A 2011 biomass resource report suggested that over 1 billion tons of dry biomass could be harvested sustainably in the United States by 2050 and that farm gate prices of $60 per dry ton are feasible (8). The predominant biomass sugars are glucose (C6) and xylose (C5), accounting for more than 90% of the fermentable sugars in plant cell walls. Microbial cofermentation of C6 and C5 sugars usually results in diauxic growth due to carbon catabolite repression, resulting in low volumetric productivity (9). Hydrogen

generation technologies, such as microbial fermentation, gasification, steam reforming, and aqueous phase reforming (6, 10–13), suffer from low product yields. For example, the hydrogen yield from microbial fermentations is limited to 4 H_2/mol of glucose. However, much higher hydrogen yields (>4 H_2/glucose) are critical to achieve their production economics because sugars usually account for more than half of biofuel production costs (14).

In vitro metabolic engineering is the construction of synthetic enzymatic pathways without cell membranes to carry out complex biochemical reactions. In addition to its fundamental role in elucidating complicated cellular metabolism and regulation (15), this field is emerging as a promising alternative biomanufacturing platform, especially for the production of low-value and high-impact biofuels and biochemicals (16–18). In vitro metabolic engineering has a number of advantages over whole-cell biosystems: high product yield without the formation of by-products or the synthesis of cell mass (19, 20); fast reaction rates, due to elimination of transport across a cell membrane (21, 22); easy product separation (21, 23); tolerance of compounds that would be toxic to intact cells (24); broad reaction conditions (25); and

Significance

Hydrogen (H_2) has great potential to be used to power passenger vehicles. One solution to these problems is to distribute and store renewable carbohydrate instead, converting it to hydrogen as required. In this work more than 10 purified enzymes were combined into artificial enzymatic pathways and a high yield from both glucose and xylose to hydrogen was achieved. Also, gaseous hydrogen can be separated from aqueous substrates easily, greatly decreasing product separation costs, and avoid reconcentrating sugar solutions. This study describes high-yield enzymatic hydrogen production from biomass sugars and an engineered reaction rate increase achieved through the use of kinetic modeling. Distributed hydrogen production based on evenly distributed less-costly biomass could accelerate the implementation of the hydrogen economy.

ENGINEERING

APPLIED BIOLOGICAL SCIENCES

nonnatural reactions, such as the enzymatic transformation of cellulose to starch (23). If the half-life times of all enzymes in an in vitro enzymatic pathway were similar to that of industrial glucose isomerase, which can produce more than 1,000,000 kg of product per kilogram of enzyme, the catalyst cost of this biotransformation would be a small fraction of product price, enabling the production of biofuels and biochemicals at very low costs (16, 26).

In this study, we demonstrate for the first time to our knowledge the production of hydrogen directly from pretreated plant biomass containing C5 and C6 sugars via in vitro metabolic engineering. In addition, a kinetic model was formulated using multiple experimental datasets and was used to optimize the overall reaction rate and hydrogen yield. The relative simplicity of in vitro synthetic enzymatic pathways compared with whole cells makes the overall system far easier to simulate and use for predictions (15). Kinetic models for enzymatic hydrogen production have been used previously to optimize the reactor design; however, experimental validation had not yet been performed (27). The problem of fitting kinetic parameters of Michaelis–Menten models to given experimental datasets was solved using a genetic algorithm (28). With an updated kinetic parameter set, optimal enzyme loading ratios were calculated, and global sensitivity analysis (GSA) (29) was applied to determine the sensitivity of each enzyme's loading over the entire range of operating conditions. Because GSA is a stochastic method, it is computationally demanding and offers advantages over traditional sensitivity analysis, where only one parameter is adjusted while the others remain constant. GSA calculates sensitivity as all parameters are varied simultaneously. This method

has been used to identify the key operating bottlenecks of kinetic and agent-based models (30, 31). Importantly, the predictions made in this research were validated experimentally, and an improved volumetric hydrogen productivity rate was achieved.

Results

Two approaches were used to demonstrate (*i*) simultaneous, high-yield utilization of C5 and C6 biomass sugars and (*ii*) rational metabolic engineering of the system for increased reaction rate through the use of a kinetic model. For high-yield biomass utilization, one mesophilic enzyme, polyphosphate glucokinase (PPGK) (discussed below), had to be used as a thermophilic source and was not available. Because activity of this enzyme significantly decreases above 40 °C (32), biomass utilization experiments were conducted at 40 °C to ensure complete conversion. For reaction rate increase experiments, a simplified pathway was used, where phosphorylation enzymes were eliminated and glucose-6-phosphate was used as the substrate. Due to the use of only thermophilic enzymes in this pathway, the reaction temperature was 50 °C for these experiments.

Pathway Design. An in vitro ATP-free synthetic enzymatic pathway was designed for the high-yield production of hydrogen from pretreated biomass sugars—glucose and xylose (Fig. 1). This pathway can be broken down into four modules: (*i*) the hydrolysis of cellulose and xylan to glucose and xylose, respectively, by using a commercial cellulase/hemicellulase mixture; (*ii*) the phosphorylation of monomer sugars glucose and xylose with polyphosphate; (*iii*) the production of reduced nicotinamide adenine dinucleotide phosphate (NADPH) and subsequently

Fig. 1. Pathway depicting the enzymatic conversion of biomass to hydrogen and CO_2. Full names of enzymes used are polyphosphate glucokinase (PPGK), xylose isomerase (XI), xylulokinase (XK), glucose 6-phosphate dehydrogenase (G6PDH), 6-phosphogluconate dehydrogenase (6PGDH), ribose 5-phosphate isomerase (R5PI), ribulose 5-phosphate epimerase (Ru5PE), transketolase (TK), transaldolase (TAL), triose phosphate isomerase (TIM), aldolase (ALD), fructose 1,6-bisphosphate (FBP), phosphoglucose isomerase (PGI), hydrogenase (H2ase), and Cellic Ctec2 cellulase (Ctec2). Details of the reactions are included in Table S1.

hydrogen by two dehydrogenases and a hydrogenase; and (*iv*) the recycling of the C5 compounds ribulose 5-phosphate and xylulose 5-phosphate to C6 glucose 6-phosphate through the nonoxidative pentose phosphate pathway, partial glycolysis, and gluconeogenesis pathways. Glucose 6-phosphate generated by the fourth module is then a substrate for the dehydrogenases in the second module. Using this pathway, theoretical yields are 12 mol of hydrogen and 6 mol of carbon dioxide per mole of glucose and 10 mol of hydrogen and 5 mol of carbon dioxide per mole of xylose.

High-Yield Hydrogen from Biomass. The most abundant agricultural residue in the United States is corn stover, which consists of leaves and stalks. It is composed of ~36% (wt/wt) cellulose and 23% (wt/wt) xylan (the main component of hemicellulose), which together account for ~92% (wt/wt) of total biomass sugars (33). To release free glucose and xylose for in vitro hydrogen production, two types of biomass pretreatments were used, cellulose solvent- and organic solvent-based lignocellulose fractionation (COSLIF) and dilute acid pretreatment (33). The pretreated biomass resulting from both procedures was then hydrolyzed by a commercial cellulase/hemicellulase mixture (Novozymes Cellic Ctec2) to maximize the release of C6 and C5 sugars.

Using the four-module in vitro enzyme cascade (Fig. 1), hydrogen was produced at high yields from corn stover hydrolyzate after both COSLIF (Fig. 2*A*) and dilute acid pretreatments (Fig. S1). The composition of each type of biomass is included in Table S2. Remarkably, there was ~100% conversion of the glucose and xylose components of the COSLIF hydrolyzate into hydrogen after 78 h at 40 °C. (Yield was calculated to be 101.87% based on hydrogen productivity data and starting hydrolyzate composition; analysis of the reaction mixture after hydrogen production indicated no detectable glucose or xylose remained.) The maximum volumetric hydrogen productivity was 2.3 mmol·L^{-1}·h^{-1}.

Due to the presence of multiple hydrogen productivity maxima, additional experiments were conducted to determine the extent to which coutilization of glucose and xylose took place. The experiments based on glucose only, xylose only, and a combination of these substrates were run under the same experimental

conditions as those based on the pretreated biomass hydrolyzate (Fig. 2*B*). All experiments were conducted on a standardized basis corresponding to relative COSLIF hydrolyzate concentrations: 2.7 mM glucose and/or 0.49 mM xylose. When glucose was the sole sugar source, maximum productivity was observed at ~1.2 h. Xylose conversion did not show a strong productivity peak, but instead exhibited a steadily increasing rate of hydrogen production. When glucose and xylose were combined, two peaks were again observed, as in the case of using the pretreated biomass. Furthermore, the initial peaks for pretreated biomass and the combination of glucose and xylose corresponded to the glucose productivity peak. These two sets of conditions also shared a second productivity peak, at 12–18 h. A similarly shaped curve also resulted when dilute acid-pretreated biomass was the sugar source (Fig. S1). Together, these results suggest that glucose and xylose were efficiently converted by the in vitro synthetic enzymatic pathway and that only small inhibitory effects, i.e., slight changes in curve shapes, were observed between the use of defined sugar substrates and the biomass hydrolyzate.

Kinetic Enzymatic Model Update and Global Sensitivity Analysis. Key metrics for the improvement of this in vitro enzymatic pathway are product yield, volumetric productivity, and minimization of the amounts of enzyme used. To probe more deeply into the rate-limiting steps, a kinetic model of a simplified pathway, consisting of only the third and fourth modules (the pentose phosphate pathway and hydrogenation, not hydrolysis and phosphorylation), was used to investigate the effects of the loading concentration of each enzyme on yield and maximum hydrogen productivity. In addition, this shortened pathway eliminated the sole mesophilic enzyme of the pathway, PPGK, allowing rate enhancement experiments to be conducted at an elevated temperature.

The kinetic model originally developed for this system described mesophilic enzymes operating at 32 °C and was built with a set of modified Michaelis–Menten equations (*SI Description of Models and Algorithms*). In the original modeling work performed by Ye et al. (34), literature values of k_{cat} and K_m were adjusted to fit experimental data. Variation of the equilibrium and inhibition constants (K_m and K_I, respectively) due to temperature was not considered here; these were held constant from the results of the previous study. Instead emphasis was placed on updating V_{max} parameters, which are the product of k_{cat}, the enzyme turnover number, and the enzyme concentration, [E]. The V_{max} parameter of each enzyme in the pathway was adjusted in this modeling study to update the model for operation at 50 °C with thermophilic enzymes. Thirteen datasets were used to develop 12 revised V_{max} parameters. After ~1,000 iterations, the genetic algorithm achieved an acceptable fit to the experimental data obtained under a variety of different enzyme loadings (Fig. S2; revised parameters are included in Table S3 and comparison with experimental values is included in Table S4).

With an updated model capable of describing a range of different enzyme loadings, GSA was conducted to determine the most important enzyme loading concentrations for maximum rate and yield of hydrogen. The results of these analyses are given in Table 1, and an in-depth description of GSA methods and their resulting indexes are given in *SI Description of Models and Algorithms*. Maximum productivity GSA results show that (*i*) the hydrogenase enzyme concentration has the greatest impact on determining the maximum rate of hydrogen production, (*ii*) G6PDH concentration has the second greatest impact, (*iii*) the concentration of 6PGDH is also relevant under certain conditions, and (*iv*) the concentrations of the other enzymes do not play a significant role in maximum rate determination. Yield-based GSA analysis also showed that the concentration of the hydrogenase enzyme had the most impact, with the transketolase having the second largest effect. However, in terms of hydrogen
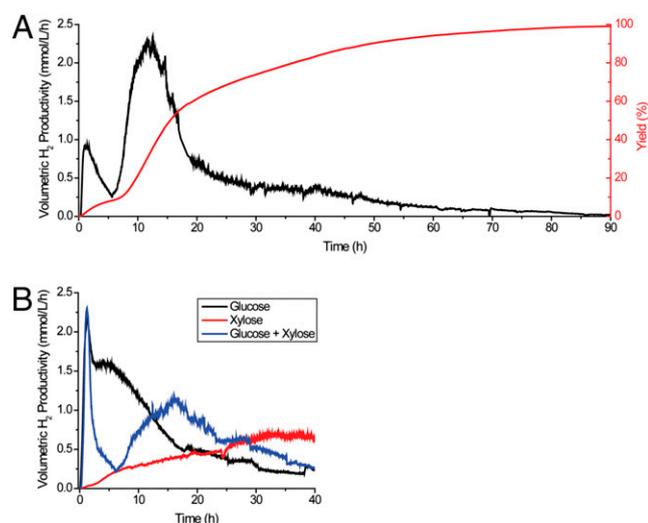

Fig. 2. (*A* and *B*) Hydrogen production from pretreated biomass (*A*) and key component sugars glucose, xylose, and a combination of the two (*B*). The shared first peak indicates initial fast rates associated with glucose utilization, due to a combination of fast phosphorylation reactions and immediate NADPH production. Initial production slows as metabolic intermediates approach equilibrium. Xylose is consumed at a slower rate, due to the increased number of enzymatic steps required to produce reducing equivalents of NADPH.

Rollin et al.

Table 1. Global sensitivity analysis results

Enzyme	Rate-based GSA		Yield-based GSA	
	S1	ST	S1	ST
G6PDH	0.305	0.418	0.044	0.188
6PGDH	0.103	0.156	0.056	0.256
Ru5PE	0.001	0	0.024	0.234
R5PI	0.001	0	0.024	0.23
TK	0.001	0	0.05	0.334
TAL	0.001	0	0.023	0.253
TIM	0.001	0	0	0.22
ALD	0.001	0	−0.005	0.001
FBP	0.001	0	−0.003	0.006
PGI	0.001	0	0.003	0.097
H2ase	0.463	0.578	0.143	0.458

S1 is the first-order sensitivity index, and ST is the total effect index. The results of two different sets of simulations are shown: the relative effect of each enzyme loading on maximum hydrogen production rate and yield.

yield almost all enzymes of the pathway had a significant albeit smaller effect (Table 1).

High-Speed Hydrogen Production: Modeling and Experimental Validation. A model simulation study was conducted where the concentration of each of the 11 enzymes was varied on a unit loading basis from 0% to 100%, with the balance of the enzyme mixture evenly divided among the other enzymes on a unit basis. The maximum rate was plotted for each set of enzyme loadings, resulting in a set of relationships showing the relative effect of each enzyme (Fig. S3). The trends for the optimum loadings for individual enzymes agreed with GSA predictions of their effects on maximum rate. Hence, although most enzymes had an optimal loading of less than 5%, both G6PDH and hydrogenase were predicted to be required in much higher loading amounts to achieve maximum hydrogen productivity. The simulation studies with these two enzymes were selected for further comparison with the experimental results to validate the updated kinetic model. Maximum rates were obtained from experiments where either G6PDH or hydrogenase loading was varied (defined as a percentage of total enzyme loading), with the balance divided evenly between the other enzymes. As shown in Fig. 3, the predicted effects of these two enzymes were confirmed, thereby validating the utility of the updated kinetic model in predicting optimal concentrations of mixtures of enzymes participating in a synthetic pathway.

A genetic algorithm was then applied to the updated kinetic model to determine optimal enzyme concentrations for the maximum hydrogen production rate. To stay within the regime where the model predicts well-defined behavior, the maximum enzyme concentrations used in the experimentally validated runs were used as upper limits. Remarkably, the resulting set of enzyme concentrations was predicted to result in a maximum rate that was three times that of the standard enzyme loadings and twice that of the highest experimental validation run. The sets of standard and optimized enzyme concentrations are included in Table S1. Importantly, the experimental results were very close to matching the predicted maximum hydrogen production rate of 32 mmol·L^{-1}·h^{-1} (Fig. 4A). This rate, threefold that of the initial case, was achieved using a substrate loading of 2 mM hexose. An additional rate increase of 69% to 54 mmol·L^{-1}·h^{-1} was achieved by increasing the total enzyme loading threefold, increasing the substrate loading to 100 mM glucose 6-phosphate, and raising the temperature from 50 °C to 60 °C (Fig. 4B).

The optimized enzyme loadings were then applied to enzymatic hydrolyzate of pretreated biomass, resulting in an increase in maximum volumetric hydrogen productivity of 45% compared

with the high-yield case (Fig. S5). Although significant, this maximum rate increase was much less than was observed for the utilization of g6p. Additional experiments showed that hydrolyzate inhibitors were responsible for a 25% reduction in maximum reaction rate (Fig. S6). These experiments are discussed in more detail in *SI Description of Models and Algorithms*.

Discussion

The future of clean energy depends on innovative breakthroughs in the design of cheap, sustainable, and efficient systems for the harvesting, conversion, and storage of renewable energy sources. Sugar-based hydrogen systems catalyzed by in vitro synthetic biosystems offer a promising solution to meet these needs. Several challenges remain for in vitro enzyme systems to become a commercially viable means of producing hydrogen from carbohydrates. These include replacing the expensive and labile cofactor NADP$^+$ with a cheap and stable biomimetic, replacing key unstable enzymes (e.g., PPGK, PGM), using cheap and abundant substrates, and achieving hydrogen production at high rate and yield. The first two challenges, use of biomimetic cofactors and improving enzyme stability, may be addressed through the discovery of more thermoenzymes, enzyme engineering, and immobilization (16, 35). This study has addressed the latter two challenges, using cheap biomass sugars in a high-yield reaction and increasing the volumetric productivity.

Volumetric productivity of hydrogen is essential to industrial scale-up. The reaction rate of 54 mmol hydrogen per hour per liter achieved here equals 3.7 W/L, ~15 times the maximum photohydrogen rate (36, 37). This productivity is comparable to those of industrial biogas and hydrogen production (13). In the past decade, in vitro enzymatic hydrogen generation has been enhanced from 0.21 mmol·L^{-1}·h^{-1} to 54 mmol·L^{-1}·h^{-1}, an improvement of more than 250-fold. It is expected that enzymatic hydrogen generation rates could be further increased by raising the reaction temperature to 80 °C or higher, using substrate-channeling synthetic metabolons (38), and through the discovery and use of more highly active enzymes and biocatalytic modules (16, 39). High-speed hydrogen production powered by
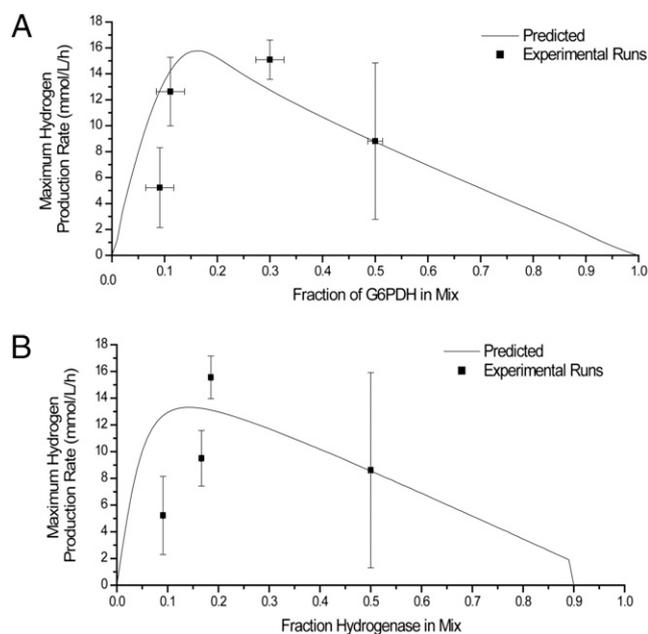

Fig. 3. (A and B) Model-predicted optimal single-enzyme loading concentrations compared with experimental data for G6PDH (A) and hydrogenase (B) (outliers removed; see Fig. S4 for complete data).
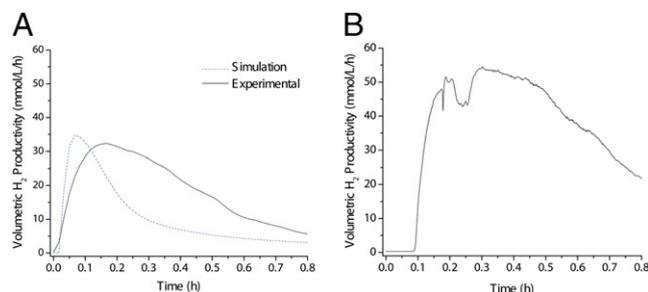
Fig. 4. (*A*) Rate enhancement was achieved by adjusting relative enzyme loadings while keeping other experimental parameters constant, as predicted by the kinetic model. (*B*) This rate was increased by a further 68% by increasing the reaction temperature, substrate loading, and cofactor concentration.

biomass-derived sugars along with independence from environmental changes such as sunlight variation (40) suggests that in vitro synthetic pathways have great potential for large-scale industrial production in the future.

The updated V_{max} kinetic parameters determined by fitting experimental data of glucose-6-phosphate to hydrogen at 50 °C were generally in agreement with previous results and literature values (34) (determined at 32 °C), although V_{max} changes for TK, TAL, and PGI were significantly different. Given the other complex and nonlinear factors affecting enzyme-catalyzed reaction rates, such as mass transport, protein–protein interactions, substrate channeling, and macromolecular crowding (41–44), the updated V_{max} values given here appear reasonable. The efficacy of this model was clear, as the maximum reaction rate was dramatically increased without changing total enzyme loading, substrate concentration, or temperature, demonstrating the utility of such models for metabolic engineering of in vitro synthetic biosystems. The use of this model with GSA also proved effective in suggesting nonobvious engineering strategies to improve both the rate and time-constrained yield of the in vitro system.

In addition to potential low-cost product separation, the production of hydrogen from enzymes in aqueous solution has another significant advantage over other biofuels—the utilization of low-concentration (and thus lower cost) sugar substrates. For example, for energy-efficient ethanol distillation, it is important to produce more than 4% (wt/vol) ethanol in the fermentation broth, meaning the initial sugar concentration should be more than 9% (wt/wt). In contrast, hydrogen gas can be separated easily from an aqueous sugar solution regardless of its concentration. There is no need for a sugar reconcentration step, which greatly reduces processing costs from biomass hydrolyzate substrates and avoids inhibition from fermentation products and/or potentially toxic compounds from biomass hydrolyzate.

Here the complete conversion of biomass sugars to hydrogen and the simultaneous coutilization of glucose and xylose by an in vitro synthetic pathway were demonstrated. In this pathway cellulose and hemicellulose were first completely converted to glucose and xylose, which in turn served as substrates for phosphorylation and hydrogen generation, using an enzyme mixture. In preliminary experiments we attempted simultaneous saccharification and hydrogen production but this required compromising the pH optimum of either the hydrogen-producing enzyme mixture (pH optimum of 7.5) or the cellulase–hemicellulase mixture (pH optimum of 4.8). Separating the two processes allowed for more careful control of each system. However, combining these process steps is a logical step forward to minimize production costs. A more advanced and likely more efficient integrated approach could make use of cello-oligomer phosphorylases. For example, a cellulase phosphorylase could use the energy of glycosidic bond hydrolysis to catalyze phosphorylation of long chain cellulose molecules, although so far such an enzyme has yet to be discovered or engineered.

Materials and Methods

Chemicals and Strains. All chemicals were reagent grade and were purchased from Sigma-Aldrich or Fisher Scientific, unless otherwise noted. Protein expression was conducted using *Escherichia coli* BL21 Star (DE3) (Invitrogen) in LB medium, with either 100 μg/mL ampicillin or 50 μg/mL kanamycin. Xylose isomerase (G4166) from *Streptomyces murinus* was purchased from Sigma. Fungal cellulase (Cellic Ctec-2) was donated by Novozymes. *Pyrococcus furiosus* hydrogenase SH1 was provided by Michael W. W. Adams (45).

Biomass Preparation. Dilute acid-pretreated corn stover was provided by the National Renewable Energy Laboratory (NREL) (Golden, CO). Dilute sulfuric acid-pretreated corn stover was produced in a pilot-scale continuous vertical reactor at 190 °C, with an acid loading of 0.048 g acid per gram dry biomass, a 1-min residence time, and a 30% (wt/wt) total solid loading, using procedures discussed elsewhere (33). COSLIF was conducted as described previously (46). Glucan and xylan contents of biomass were determined using the modified NREL laboratory analysis procedure for the determination of structural carbohydrates in biomass (47). Enzymatic hydrolysis was conducted separately, before in vitro conversion to hydrogen, according to the NREL laboratory analytical procedure entitled "enzymatic saccharification of lignocellulose biomass."

Production and Purification of Recombinant Enzymes. All enzymes used in this study (and their abbreviations) are listed in Table S1. Expression vectors were incorporated by heat shock, and colonies were grown on agar plates with the appropriate antibiotic overnight. Colonies were chosen for inoculation in 5 mL LB seed cultures and cell growth was conducted at 37 °C overnight. Seed cultures were used as 1% inoculum in 200 mL LB cultures containing 50 μg/mL kanamycin or 100 μg/mL ampicillin. Cultures were incubated at 37 °C in a rotary shaker at 250 rpm until absorbance at 600 nm reached 0.6–0.8, at which point protein expression was induced by adding isopropyl-β-D-thiogalactopyranoside (IPTG) to a final concentration of 0.01–0.1 mM. Expression was conducted at 37 °C for 4 h or at 18 °C for 20 h. Cells were centrifuged at 4 °C, washed twice with 50 mM Tris·HCl buffer (pH 7.5), and resuspended in 15 mL of 30 mM Hepes buffer (pH 7.5) containing 0.5 M NaCl and 1 mM EDTA. Cell lysis was conducted using sonication in an ice bath. Lysate was centrifuged, and target proteins were recovered from the supernatant using His-tag purification, CBM-intein self-cleavage, ethylene glycol elution of CBM-tagged enzyme, or heat treatment. For additional purification and enzyme activity assay details, see Table S1 (20, 48).

In Vitro Enzyme Mixture. Biomass and g6p conversion experiments were carried out using the enzyme loadings listed in Table S1. All enzymes were stored in 50% (wt/wt) glycerol at −20 °C, except for xylose isomerase, which was stored at 4 °C. To prepare for the reaction, appropriate volumes of each purified enzyme were combined and diluted to 0.1% glycerol with the addition of 20 mM Hepes buffer (pH 7.0) and then reconcentrated with 10,000 MWCO Amicon centrifuge filters from Millipore. Final reaction buffer was adjusted to a 100-mM Hepes (pH 7.5) buffer containing 4 mM NADP$^+$, 0.5 mM thyamine pyrophosphate, 10 mM MgCl$_2$, 0.5 mM MnCl$_2$. and 4 mM polyphosphate [$(P_i)_6$, sodium hexametaphosphate]. A total of 28 mg of immobilized XI per 1 mL of the reaction volume was placed in the reaction vessel, followed by addition of all enzymes plus final reaction buffer. To protect against microbial growth, 50 μg/mL of kanamycin was added. Substrate (enzymatic biomass hydrolyzate or g6p) was added to start the reaction. Pretreated biomass was added as a slurry and g6p was added in solution. All reactions were conducted at an end substrate concentration of 2 mM g6p or a loading of approximately equivalent theoretical hydrogen yield of 2 mM glucose, for pretreated biomass. The reactor was sealed and the solution was agitated with a magnetic stir bar. Temperature, carrier gas flow rate, and hydrogen signal were monitored continuously throughout all experiments.

System for Hydrogen Detection. Experiments were conducted in a continuous-flow system purged with 30 mL/min ultrapure nitrogen (Airgas). Hydrogen evolution was detected with a tin oxide thermal conductivity sensor (Figaro TGS 822) previously calibrated with in-line flow controllers and ultrapure hydrogen (Airgas) (20, 48). For biomass conversion, the reactor and condenser were maintained at 40 °C and 21 °C, respectively, which were controlled by recirculation thermal baths of distilled water (Fisher Scientific; Isotemp Refrigerated Circulator Bath Model 3016D). For g6p experiments, the reactor and condenser were maintained at 50 °C and 19 °C, respectively. Data acquisition was

Rollin et al.

conducted with a DAQ USB-6210 (National Instruments) and analyzed by Lab-View SignalExpress 2009 (National Instruments).

Kinetic Model, Genetic Optimization, and Global Sensitivity Analysis. The kinetic model used here was originally developed by Ye et al. (34). New kinetic parameters were calculated by minimizing the difference between 13 sets of experimental data and simulated hydrogen production under the same respective conditions. Experimental runs were conducted with a loading of 1 unit/mL reactor volume (standard conditions), as well as each of the following separate variations: 10 units/mL G6PDH, 2 units/mL hydrogenase, 2 units/mL R5PI, 2 units/mL Ru5PE, 2 units/mL TAL, 2 units/mL TIM, 2 units/mL ALD, and 30% G6PDH (in this last case, this translates to 3.3 units/mL G6PDH and 0.77 units/mL of all other enzymes). A genetic algorithm was used to determine the best fit of the kinetic parameters. Details of the algorithm are as follows: Generations contained 30 chromosomes (each of which contained a vector of kinetic parameters, referred to as genes for this discussion), BLX-α crossover and nonuniform mutation operators were used to exchange genetic information and create new chromosomes (50% of the population), the top 25% of the population was reproduced, and 25% of each population was generated randomly. The genetic algorithm was run for 1,000 generations, which was more than sufficient to achieve convergence.

In GSA, stochastic simulations were used to calculate model output (hydrogen production rate or yield) based on inputs (enzyme loading amounts) over the entire range of parameter values. Then each input was assessed using a variance-based method (31), wherein the contribution of each input parameter to the total variance of the output was used to estimate global sensitivity. GSA calculates first-order (S1) and total effect (ST) indexes. The former describes the global influence of the variable itself, and the latter takes into account interactions with all other variables (29). Both algorithms are discussed in further detail in *SI Description of Models and Algorithms*. All calculations were performed using MATLAB (R2013A) (MathWorks).

1. Navarro RM, Peña MA, Fierro JLG (2007) Hydrogen production reactions from carbon feedstocks: Fossil fuels and biomass. *Chem Rev* 107(10):3952–3991.
2. Haynes CA, Gonzalez R (2014) Rethinking biological activation of methane and conversion to liquid fuels. *Nat Chem Biol* 10(5):331–339.
3. Norskov JK, Christensen CH (2006) Chemistry. Toward efficient hydrogen production at surfaces. *Science* 312(5778):1322–1323.
4. Kim TW, Choi K-S (2014) Nanoporous BiVO$_4$ photoanodes with dual-layer oxygen evolution catalysts for solar water splitting. *Science* 343(6174):990–994.
5. Esswein AJ, Nocera DG (2007) Hydrogen production by molecular photocatalysis. *Chem Rev* 107(10):4022–4047.
6. Armaroli N, Balzani V (2011) The hydrogen issue. *ChemSusChem* 4(1):21–36.
7. Chapin DM, et al. (2013) *Transitions to Alternative Vehicles and Fuels* (National Academies Press, Washington, DC).
8. Perlack RD, Stokes BJ (2011) *U.S. Billion-Ton Update: Biomass Supply for a Bioenergy and Bioproducts Industry,* ORNL/TM-2011/224 (Department of Energy, Oak Ridge National Laboratory, Oak Ridge, TN), p 227.
9. Farwick A, Bruder S, Schadeweg V, Oreb M, Boles E (2014) Engineering of yeast hexose transporters to transport D-xylose without inhibition by D-glucose. *Proc Natl Acad Sci USA* 111(14):5159–5164.
10. Castello D, Fiori L (2011) Supercritical water gasification of biomass: Thermodynamic constraints. *Bioresour Technol* 102(16):7574–7582.
11. Maeda T, Sanchez-Torres V, Wood TK (2012) Hydrogen production by recombinant *Escherichia coli* strains. *Microb Biotechnol* 5(2):214–225.
12. Cortright RD, Davda RR, Dumesic JA (2002) Hydrogen from catalytic reforming of biomass-derived hydrocarbons in liquid water. *Nature* 418(6901):964–967.
13. Kotay SM, Das D (2008) Biohydrogen as a renewable energy resource–Prospects and potentials. *Int J Hydrogen Energy* 33:258–263.
14. Lynd LR, Wyman CE, Gerngross TU (1999) Biocommodity engineering. *Biotechnol Prog* 15(5):777–793.
15. Jung GY, Stephanopoulos G (2004) A functional protein chip for pathway optimization and in vitro metabolic engineering. *Science* 304(5669):428–431.
16. Rollin JA, Tam W, Zhang Y-HP (2013) New biotechnology paradigm: Cell-free biosystems for biomanufacturing. *Green Chem* 15:1708–1719.
17. Billerbeck S, Härle J, Panke S (2013) The good of two worlds: Increasing complexity in cell-free systems. *Curr Opin Biotechnol* 24(6):1037–1043.
18. Harris DC, Jewett MC (2012) Cell-free biology: Exploiting the interface between synthetic biology and synthetic chemistry. *Curr Opin Biotechnol* 23(5):672–678.
19. Opgenorth PH, Korman TP, Bowie JU (2014) A synthetic biochemistry molecular purge valve module that maintains redox balance. *Nat Commun* 5:4113.
20. Martín del Campo JS, et al. (2013) High-yield production of dihydrogen from xylose by using a synthetic enzyme cascade in a cell-free system. *Angew Chem Int Ed Engl* 52(17):4587–4590.
21. Hodgman CE, Jewett MC (2012) Cell-free synthetic biology: Thinking outside the cell. *Metab Eng* 14(3):261–269.
22. Zhu Z, Kim Tam T, Sun F, You C, Percival Zhang YH (2014) A high-energy-density sugar biobattery based on a synthetic enzymatic pathway. *Nat Commun* 5:3026.
23. You C, et al. (2013) Enzymatic transformation of nonfood biomass to starch. *Proc Natl Acad Sci USA* 110(18):7182–7187.
24. Guterl J-K, et al. (2012) Cell-free metabolic engineering: Production of chemicals by minimized reaction cascades. *ChemSusChem* 5(11):2165–2172.
25. Panke S, Held M, Wubbolts M (2004) Trends and innovations in industrial biocatalysis for the production of fine chemicals. *Curr Opin Biotechnol* 15(4):272–279.
26. Tufvesson Pr, Lima-Ramos J, Nordblad M, Woodley JM (2011) Guidelines and cost analysis for catalyst production in biocatalytic processes. *Org Process Res Dev* 15(1):266–274.
27. Ardao I, Zeng A-P (2013) In silico evaluation of a complex multi-enzymatic system using one-pot and modular approaches: Application to the high-yield production of hydrogen from a synthetic metabolic pathway. *Chem Eng Sci* 87:183–193.
28. Holland JH (1975) *Adaptation in Natural and Artificial Systems: An Introductory Analysis with Applications to Biology, Control, and Artificial Intelligence* (Univ of Michigan Press, Ann Arbor, MI).
29. Saltelli A, et al. (2008) *Global Sensitivity Analysis: The Primer* (Wiley, Chichester, West Sussex, England).
30. Apte AA, Senger RS, Fong SS (2014) Designing novel cellulase systems through agent-based modeling and global sensitivity analysis. *Bioengineered* 5(4):243–253.
31. Ogejo JA, Senger R, Zhang R (2010) Global sensitivity analysis of a process-based model for ammonia emissions from manure storage and treatment structures. *Atmos Environ* 44(30):3621–3629.
32. Liao H, Myung S, Zhang Y-HP (2012) One-step purification and immobilization of thermophilic polyphosphate glucokinase from *Thermobifida fusca* YX: Glucose-6-phosphate generation without ATP. *Appl Microbiol Biotechnol* 93(3):1109–1117.
33. Zhu Z, et al. (2009) Comparative study of corn stover pretreated by dilute acid and cellulose solvent-based lignocellulose fractionation: Enzymatic hydrolysis, supramolecular structure, and substrate accessibility. *Biotechnol Bioeng* 103(4):715–724.
34. Ye X, et al. (2009) Spontaneous high-yield production of hydrogen from cellulosic materials and water catalyzed by enzyme cocktails. *ChemSusChem* 2(2):149–152.
35. Paul CE, Arends IWCE, Hollmann F (2014) Is simpler better? Synthetic nicotinamide cofactor analogues for redox chemistry. *ACS Catal* 4:788–797.
36. Argun H, Kargi F (2011) Bio-hydrogen production by different operational modes of dark and photo-fermentation: An overview. *Int J Hydrogen Energy* 36(13):7443–7459.
37. Michel H (2012) Editorial: The nonsense of biofuels. *Angew Chem Int Ed Engl* 51(11):2516–2518.
38. You C, Myung S, Zhang Y-HP (2012) Facilitated substrate channeling in a self-assembled trifunctional enzyme complex. *Angew Chem Int Ed Engl* 51(35):8787–8790.
39. Bräsen C, Esser D, Rauch B, Siebers B (2014) Carbohydrate metabolism in Archaea: Current insights into unusual enzymes and pathways and their regulation. *Microbiol Mol Biol Rev* 78(1):89–175.
40. Jones ME, Banholzer WF (2014) Solar flux, water, and land impose limits on biology. *Biotechnol Bioeng* 111(6):1059–1061.
41. Srivastava DK, Bernhard SA (1987) Biophysical chemistry of metabolic reaction sequences in concentrated enzyme solution and in the cell. *Annu Rev Biophys Biophys Chem* 16(1):175–204.
42. Ge X, Luo D, Xu J (2011) Cell-free protein expression under macromolecular crowding conditions. *PLoS ONE* 6(12):e28707.
43. Wienkers LC, Heath TG (2005) Predicting in vivo drug interactions from in vitro drug discovery data. *Nat Rev Drug Discov* 4(10):825–833.
44. Srivastava DK, Bernhard SA (1986) Metabolite transfer via enzyme-enzyme complexes. *Science* 234(4780):1081–1086.
45. Chandrayan SK, et al. (2012) Engineering hyperthermophilic archaeon *Pyrococcus furiosus* to overproduce its cytoplasmic [NiFe]-hydrogenase. *J Biol Chem* 287(5):3257–3264.
46. Rollin JA, Zhu Z, Sathitsuksanoh N, Zhang Y-HP (2011) Increasing cellulose accessibility is more important than removing lignin: A comparison of cellulose solvent-based lignocellulose fractionation and soaking in aqueous ammonia. *Biotechnol Bioeng* 108(1):22–30.
47. Moxley G, Zhang Y-HP (2007) More accurate determination of acid-labile carbohydrate composition in lignocellulose by modified quantitative saccharification. *Energy Fuels* 21:3684–3688.
48. Myung S, et al. (2014) In vitro metabolic engineering of hydrogen production at theoretical yield from sucrose. *Metab Eng* 24(1):70–77.